ACADEMIC
PRESS

Characterization of cis-acting sequences involved in packaging porcine adenovirus type 3[1]

Li Xing and Suresh Kumar Tikoo*

Vaccine and Infectious Disease Organization, University of Saskatchewan, Saskatoon, Saskatchewan, Canada S7N 5E3

Abstract

Encapsidation of adenovirus DNA involves specific interactions between *cis*-acting genomic DNA sequences and *trans*-acting proteins. The *cis*-acting packaging domain located near the left inverted terminal repeat is composed of a series of redundant but not functionally equivalent motifs. Such motifs are made up of the consensus sequence 5′-TTTGN$_8$CG-3′ and 5′-TTTG/A-3′ in human adenovirus 5 (HAV-5) and canine adenovirus-2 (CAV-2), respectively. To gain comparative insight into adenovirus encapsidation, we examined the packaging domain of porcine adenovirus-3 (PAV-3). Using deletion mutants, we localized the PAV-3 packaging domain to 319 bp (nt 212 to 531), which contains six *cis*-acting elements. However, this domain does not contain the consensus motifs identified in HAV-5. In addition, consensus motif found in CAV-2 is present only once in PAV-3. Instead, PAV-3 packaging domain appears to contain AT/GC-rich sequences. The packaging motifs of PAV-3, which are functionally redundant but not equivalent, are located at the left end of the genome. © 2003 Elsevier Inc. All rights reserved.

Since adenoviruses have become popular as vectors for the delivery of foreign genes in mammalian cells, constant attempts are being made to develop adenovirus vectors with improved capacity, safety, and efficacy (Russell, 2000). To achieve this, detailed knowledge of biology of adenovirus including mechanisms of virus particle assembly and viral DNA packaging is necessary. Although analysis of adenovirus particle assembly has been the focus of many studies (D'Halluin et al., 1978a, 1978b, 1980; Edvardsson et al., 1976, 1978), little is known about the basic mechanism of encapsidation of adenovirus DNA.

Earlier studies using temperature-sensitive mutants and pulse-chase kinetics experiments have established that adenovirus DNA is inserted into preformed, empty capsids late in the viral life cycle (D'Halluin, 1995). Other studies on viral incomplete particles containing DNA molecules of subgenomic length suggested that DNA packaging occurs in a polar fashion from left to right (Daniell, 1976; Tibbetts, 1977; Hammarskjold and Winberg, 1980; Kosturko et al.,

1982; Robinson and Tibbetts, 1984). Subsequent studies suggested that a *cis*-acting packaging domain located in the left end of the adenovirus genome is required for the selective encapsidation of viral DNA (Grable and Hearing, 1990, 1992; Hearing et al., 1987). However, the position and the orientation of this packaging domain is not strict as long as it is within first or last 600 bp (Hasson et al., 1989; Hearing and Shenk, 1983; Hearing et al., 1987).

The *cis*-acting packaging domain in human adenovirus type 5 (HAV-5) is located in the left end 380 bp (Hearing et al., 1987). It contains at least seven functionally redundant "A-repeat" domains (Grable and Hearing, 1990, 1992), four of which (AI, AII, AV, and AVI) are most dominant (Schmid and Hearing, 1997). Mutational analysis of A-repeat consensus sequence (5′-TTTGN$_8$CG-3′) suggested that sequence as well as the spacing (N$_8$) of two elements 5′-TTTG-3′ and 5′-CG-3′ are critical for maximum packaging capacity (Schmid and Hearing, 1997). In addition to *cis*-acting sequences, a number of viral and/or cellular proteins are thought to be involved in adenovirus DNA packaging (Fujisawa and Hearing, 1994; Grable and Hearing, 1992; Schmid and Hearing, 1995). Schmid and Hearing have detected some cellular proteins binding to the packaging sequences (Schmid and Hearing, 1997). Among viral pro-

* Corresponding author. 120 Veterinary Road, University of Saskatchewan, Saskatoon, SK, Canada S7N 5E3. Fax: +306-966-7478.

E-mail address: Tikoo@Sask.Usask.ca (S.K. Tikoo).

A.

```
CATCATCAATAATATACCGCACACTTTTATTGCCCCTTTTGTGGCGTGGTGATTGGCGGA    60

GAGGGTTGGGGGCGGCGGGCGGTGATTGGTGGAGAGGGGTGTGACGTAGCGTGGGAACGT   120

GACGTCGCGTGGGAAAATGACGTGTGATGACGTCCCGTGGGAACGGGTCAAAGTCCAAGG   180

GGAAGGGGTGGAGCCCTGGGGCGGTCCTCCGCGGGGCGGGGCCGAGCGGCGG**AAATT**CCC   240

GCACAGGTGGAGAGTACCGCGGG**ATTTT**GTGCCCTCTGGACCGGACCTTCGCCCTCCGGT   300

GTGGCACTTCCGCACCACACGTCCGCGGCCCGG**TATT**CCCCACCTGACGACGGTGACACC   360

ACTCACCTGAGCGGGGTGTCCTTCGCGCTGAGAGGTCCGCGGCGGCCGCCCGAGATGACG   420

TGTGTGGGTG**TATTTTTT**CCCCTCAGTG**TATATA**GTCCGCGCAGCGCCCGAGAGTC**A**CTA   480

CTCTTGAGTCCGAAGGGAGTAGAG**TTTT**CTCTCAGCGGAACAGACCCTCGAC**ATG**GCGAA   540

CAGACTTCACCTGGACTGGG                                          560
```

B.

```
CCGCCCAGAAGTCCCGGGAATTCCCGCCAGCCGGCTCCGCCGCGACCTGCGAC**TTTG**ACC   33920

CCGCCCCTCGGAC**TTTG**ACCGTTCCCACGCCGTTCCACGTCATTTTCCCACGCGACGTCA   33980

CCACGCTACGTCACACCCCTCTCCACCAATCACCGCCCGCCGCCCCCAACCCTCTCCGCC   34040

AATCACCACGCCACAAAAGGGGCAATAAAAGTGTGCGGTATATTATTGATGATG        34094
```

Fig. 1. Nucleotide sequence of PAV-3 termini. Numbers indicate the nucleotide position relative to the left terminus of PAV-3 genome. Inverted terminal repeat (ITR) nucleotide sequence is shown in italic. (A) Nucleotide sequence of left terminus. The cap site A and ATG codon for E1A gene are shown in italic bold case. AT-rich regions are in bold case. (B) Nucleotide sequence of PAV-3 right terminus. TTTG motif is shown in bold case.

teins, the 52/55-kDa and IVa2 proteins have been shown to date to be required for viral DNA packaging (Gustin and Imperiale, 1998; Hasson et al., 1989; Zhang et al., 2000, 2001). Interaction of IVa2 with the different components of the DNA packaging machinery has been shown to be serotype specific (Zhang et al., 2000, 2001). Although identity of some of these proteins is becoming known, the nature of interactions between different components of the packaging machinery remains unclear.

Recently, *cis*-acting packaging domain of canine adenovirus-2 (CAV-2) has been identified (Soudais et al., 2001). Similar to HAV-5 (Schmid and Hearing, 1997), *cis*-acting packaging motifs of CAV-2 are located in the left end of the genome and are functionally redundant (Soudais et al., 2001). However, the primary sequence of packaging motifs required for packaging CAV-2 or HAV-5 DNA appears to be different (Schmid and Hearing, 1997; Soudais et al., 2001). By identifying the *cis*-acting packaging domain of adenoviruses infecting different species, we may be able to identify different *trans*-acting factors involved in adenovirus packaging, thus clarifying the general mechanism of adenovirus packaging. In addition, availability of *cis*-acting packaging domain of PAV-3 may help in the construction of hybrid (PAV-3/HAV-5) gutless adenovirus vectors, thus helping to eliminate or substantially reduce the helper virus contamination. In the present study, we identified the packaging domain of porcine adenovirus 3 (PAV-3) by constructing and analyzing packaging deletion mutants.

Results

Analysis of the PAV-3 genomic sequences

The *cis*-acting packaging domain of canine adenovirus-2 (Soudais et al., 2001) and most human adenoviruses (Grable and Hearing, 1990, 1992; Hammarskjold and Winberg, 1980; Hearing et al., 1987; Kosturko et al., 1982; Schmid and Hearing, 1997) appears to be located near the left end of the genome between inverted terminal repeat (ITR) and the start of E1A coding region. However, the position and orientation of the packaging domain is not strict as long as it is within the first or the last 600 bp of the genome (Hammarskjold and Winberg, 1980; Hearing and Shenk, 1983; Hearing et al., 1987). The ITR of PAV-3 is 144 bp in length (Reddy et al., 1998a). Based on the consensus sequences of *cis*-acting packaging motif of human adenovirus 5 [5′-TTTGN$_8$CG-3′] (Schmid and Hearing, 1997), we searched PAV-3 genome for putative *cis*-acting packaging motifs in two regions of the viral genome (between left ITR and E1A gene and between right ITR and E4 region). We could not find any motif that showed perfect homology with the consensus packaging motifs of HAV-5 between left ITR and E1A gene or between right ITR and E4 region of PAV-3 (Fig. 1). However, there are six AT/GC-rich motifs between left ITR and E1A coding sequence of PAV-3 (Fig. 1). In addition, there are two AT/GC-rich motifs containing "TTTG" sequence between right ITR and E4 region of
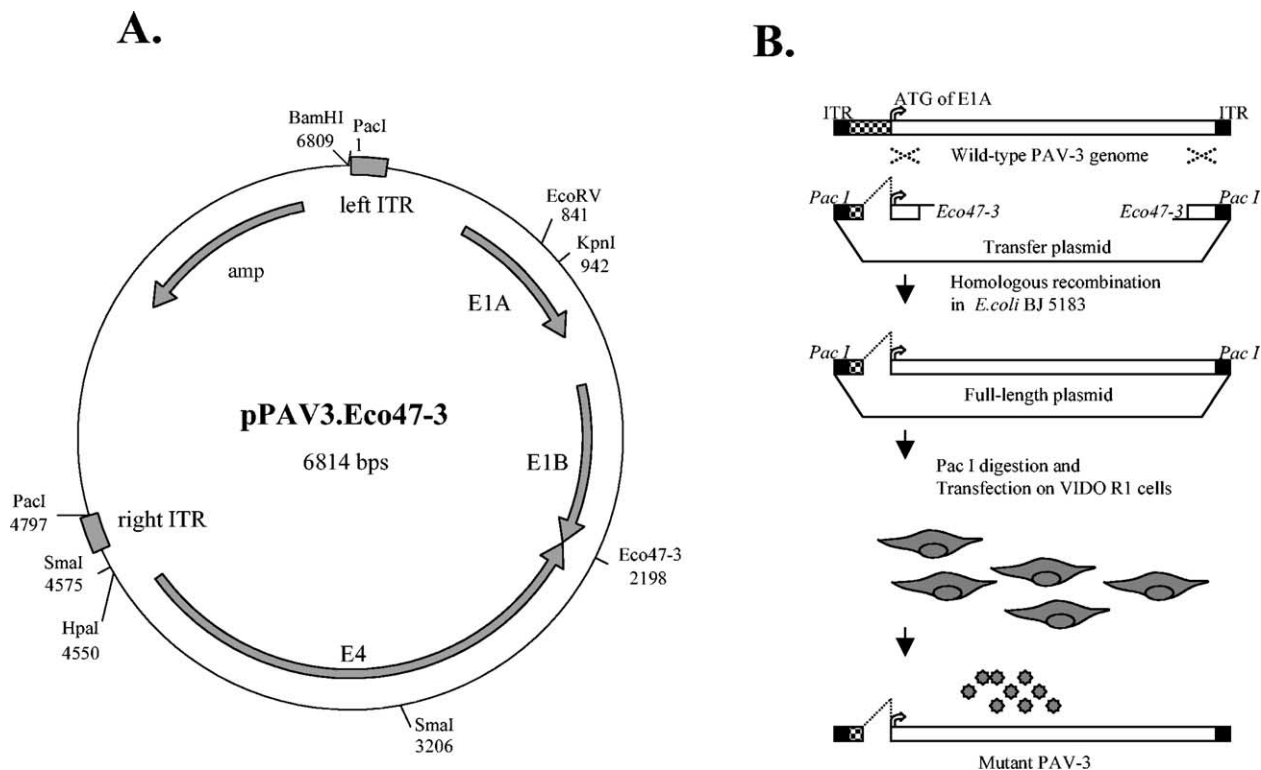
A.

B.

Fig. 2. Schematic diagram showing isolation of mutant PAV-3. (A) Plasmid pPAV3.Eco47-3 used for producing deletion mutations. The left and right ITRs of PAV-3 are indicated by filled boxes. PAV-3 sequences are from the extreme left (nt 1 to 2192) and right (nt 31499 to 34094) ends of the viral genome. The E1A, E1B, and E4 coding regions, and their directions of transcription, are shown by filled arrows. (B). Strategy used for the construction of full-length plasmid and isolation of mutant virus. The deletion mutations were created initially in the transfer plasmid pPAV3.Eco47-3 using PCR. Plasmid DNA (thin line); PAV-3 genomic DNA (open box); ITR (filled box); deleted region (hatched boxes).

PAV-3 (Fig. 1). To characterize which of them could function in *cis* as packaging motifs for PAV-3 DNA, deletion mutations were introduced into intact viral genome to delete these candidate motifs in single fashion or in combinations.

Isolation of mutant viruses

To define *cis*-acting sequences required for packaging PAV-3 DNA, initially, deletion mutations were constructed in a recombinant transfer plasmid pPAV3.Eco47-3 (Fig. 2A) by replacing DNA sequences located between *Bam*HI-*Eco*RV restriction enzyme sites or between *Hpa*I-*Pac*I restriction enzyme sites with two PCR DNA fragments in a three-way ligation. The individual deletions were then introduced into intact viral genome (Fig. 2B) by homologous recombination between wild-type PAV-3 genomic DNA and Eco47-3-linearized individual recombinant transfer plasmid in *Escherichia coli* BJ5183 cells (Chartier et al., 1996). The *Pac*I-digested individual full-length plasmid DNA, transfected into VIDO R1 cells, produced cytopathic effects (CPE) in 14 to 21 days. The infected cell monolayers showing 50% cytopathic effects were collected and freeze-thawed, and recombinant viruses were plaque purified and propagated in VIDO R1 cells.

To confirm the presence of specific deletion(s), we analyzed the genomic DNA by PCR using primers generated from the flanking regions of the deletions (Table 1). Mutant viral DNAs were PCR amplified using primer pairs PSR32-P2 for deletions between left ITR and E1A gene (Fig. 3A, C, D, and E) or PR1-PSR32 for deletions between E4 region and right ITR (Fig. 3B) and observed for a shift in the size of their products generated due to deletions in the mutants, compared to wild-type PAV-3 DNA (Fig. 3). Compared to the wild-type PAV-3, all the deletion mutants yielded the expected amplification products. Finally, the identity of each deletion was confirmed by DNA sequence analysis of the PCR fragments amplified using mutant viral DNA(s).

Analysis of mutant viruses with internal deletions

Most of deletion mutations in this study were located between nucleotide (nt) position 151 and 531, which also contain the regulatory region of PAV-3 E1A transcription unit (Reddy et al., 1998a). The mutation in this region could probably affect the expression of E1A gene and thus result in the changes in viral growth of mutant PAV-3, or even make the virus nonviable. Since VIDO R1 cells could complement the E1A defect of PAV-3 (Reddy et al., 1999b), this cell line was used throughout this study.

Table 1
Primers used in PCR

Primer	Sequence[a]	PAV-3 nucleotide position[b]	Description
P1	5′-CGT CTT CAA <u>GGA TCC</u> TTA-3′	minus 23–minus 5	Sense, *Bam*HI
P2	5′-CGC GCT <u>GAT ATC</u> CTC CTC-3′	827–844	Antisense, *Eco*RV
P3	5′-CCG <u>CAA TTG</u> GTC ATC ACA CGT CAT TTT C-3′	133–151	Antisense, *Mfe*I
P4	5′-CCG <u>CAA TTG</u> GGG GCG GGG CCG AGC GGC-3′	213–230	Sense, *Mfe*I
P5	5′-CCG <u>CAA TTG</u> GCG GAG GAC CGC CCC AGG-3′	195–212	Antisense, *Mfe*I
P6	5′-CCG <u>CAA TTG</u> ATA CCG CGG GAT TTT GT-3′	255–271	Sense, *Mfe*I
P7	5′-CCG <u>CAA TTG</u> CTC CAC CTG TGC GGG AAT-3′	235–252	Antisense, *Mfe*I
P8	5′-CCG <u>CAA TTG</u> CAC CAC ACG TCC GCG G-3′	313–328	Sense, *Mfe*I
P9	5′-CCG <u>CAA TTG</u> CGG AAG TGC CAC ACC GGA-3′	295–312	Antisense, *Mfe*I
P10	5′-CCG <u>CAA TTG</u> TCG CGC TGA GAG GTC CGC G-3′	383–401	Sense, *Mfe*I
P11	5′-CCG <u>CAA TTG</u> AGG ACA CCC CGC TCA GGT-3′	365–382	Antisense, *Mfe*I
P12	5′-CCG <u>CAA TTG</u> TTT TTT CCC CTC AGT GTA TA-3′	433–452	Sense, *Mfe*I
P13	5′-CCG <u>CAA TTG</u> TAC ACC CAC ACA CGT CAT-3′	415–432	Antisense, *Mfe*I
P14	5′-CCG <u>CAA TTG</u> TAT ATA GTC CGC GCA-3′	449–463	Sense, *Mfe*I
P15	5′-CCG <u>CAA TTG</u> ACT GAG GGG AAA AAA TAC-3′	430–447	Antisense, *Mfe*I
P16	5′-CCG <u>CAA TTG</u> GTC ACT ACT CTT GAG TCC-3′	474–491	Sense, *Mfe*I
P17	5′-CCG <u>CAA TTG</u> CGC GGA CTA TAT ACA CTG-3′	444–461	Antisense, *Mfe*I
P18	5′-CCG <u>CAA TTG</u> GAG TAG AGT TTT CTC TCA-3′	497–514	Sense, *Mfe*I
P19	5′-CCG <u>CAA TTG</u> CTT CGG ACT CAA GAG TAG-3′	478–495	Antisense, *Mfe*I
P20	5′-CCG <u>CAA TTG</u> ACA TGG CGA CAC GAC TTC-3′	531–548	Sense, *Mfe*I
PR1	5′-CCG CCT CCG <u>CGT TAA C</u>GA TTA ACC-3′	33838–33861	Sense, *Hpa*I
PR2	5′-AGC TT<u>T TAA TTA </u>ACA TCA TC-3′	34088–34094	Antisense, *Pac*I
PR3	5′-CCG <u>CAA TTG</u> CGC AGG TCG CGG CGG AGC-3′	33894–33911	Antisense, *Mfe*I
PR4	5′-CCG <u>CAA TTG</u> CCT CGG ACT TTG ACC GT-3′	33926–33942	Sense, *Mfe*I
PR5	5′-CCG <u>CAA TTG</u> GGC GGG GTC AAA GTC GCA-3′	33908–33926	Antisense, *Mfe*I
PR6	5′-CCG <u>CAA TTG</u> CCA CGT CAT TTT CCC A-3′	33949–33965	Sense, *Mfe*I
PSR32	5′-CGG CGG GAT CCT TAA TTA ACA TCA TCA ATA ATA TAC CGC ACA CTT TT-3′	1–18	

[a] The restriction endonuclease cleavage sites are underlined.

[b] Numbers indicate the nucleotide position relative to the left terminus of PAV-3 (Reddy et al., 1998b) genome. PAV-3 nucleotide sequences are indicated in boldface type.

To analyze the efficiency of packaging of the mutant viral DNA, we used two assays. First, we determined the yield of infectious virus in single infection on VIDO R1 cells by plaque assay. Since deletion of part of E1A region of PAV-3 genome has been shown to lead to reduced virus yield in VIDO R1 cells (Reddy et al., 1999b), we also used a coinfection assay. In this assay, VIDO R1 cells were coinfected with wild-type and mutant PAV-3 at the same m.o.i. At 2 days after infection, one-half of the cells were used to isolate the high-molecular-weight nuclear DNA and the other half of the cells were used to isolate the viral DNA from virion particles (Grable and Hearing, 1990, 1992). The coinfecting viral genomes could be distinguished by digestion of viral DNA with *Mfe*I and *Kpn*I and by subsequent Southern hybridization analysis.

In the first set of mutant viruses, the small deletions were targeted at the left (Fig. 4A; nt 151 to 531) and right (Fig. 4A; nt 33911 to 33949) end of PAV-3 genome. As seen in Fig. 4, the results of the single infection in VIDO R1 cells showed that deletions extending from nt 151 to 213, 212 to 254, 252 to 313, 312 to 383, 432 to 449, and 461 to 497 resulted in two- to sevenfold reduction in the yield of PAV-3. However, in coinfection assays (Fig. 4B), deletions extending from nt 151 to 213 and 461 to 497 had no effect on the packaging abilities of mutant viruses (Fig. 4A). In addition, deletions extending from 382 to 433 had no effects on the yield of PAV-3 in single infection as well as packaging ability of the virus in coinfection assays (Fig. 4A). These results suggested that these regions do not contain packaging motif(s). In contrast, the changes in packaging efficiency in coinfection assays (Fig. 4B) were evident with mutant viruses containing deletions between nt 212 and 254 (Pav3-212/254), nt 252 and 313 (Pav3-252/313), nt 312 and 383 (Pav3-312/383), nt 432 and 449 (Pav3-432/449), nt 447 and 474 (Pav3-447/474), and nt 495 and 531 (Pav3-495/531). However, the mutant viruses containing deletions between nt 33911 to 33949 at the right end of viral genome grew as well as wild-type virus in VIDO R1 cells in single infection (Fig. 4A). These results suggested that the packaging domains of PAV-3 are (a) located at the left end of viral genome, (b) possibly functionally redundant as described for human adenovirus type 5 (Grable and Hearing, 1990; 1992; Schmid and Hearing, 1997), and (c) appeared to overlap the promoter region of E1A gene.
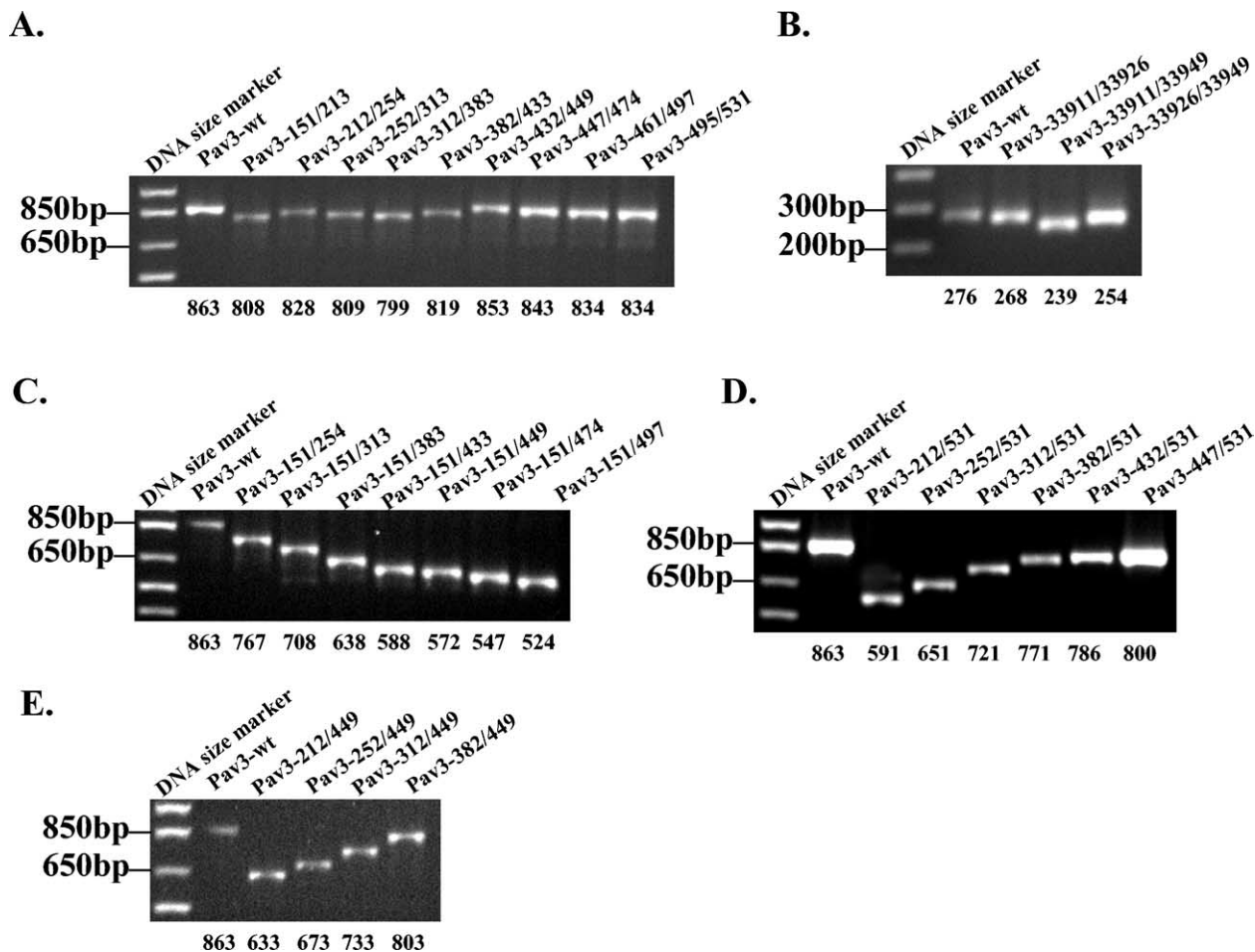
Fig. 3. Genomic PCR of viral mutants. PCR amplified products generated by primer pair PSR32-P2 (A,C,D,E) or PSR32-PR1 (B) flanking the individual deletions are shown in comparison to PCR products generated by amplification of the same region from wild- type PAV-3 DNA. The expected sizes of amplified products generated by PCR from wild-type PAV-3 and mutant viruses are shown at the bottom. Molecular size markers are indicated on the left.

Analysis of mutant viruses with progressive deletions

To further define the packaging domain of PAV-3, we constructed two additional sets of mutant viruses. One set of mutant viruses contains deletions, which progress from a common site at nt 151 toward the downstream border of the packaging domain (Fig. 5A). As seen in Fig. 5, mutant Pav3-151/254 carrying deletion between nt 151 and 254 had a twofold reduction in virus yield in single infection and a twofold reduction in the packaging ability in coinfection assays. The sequential additional deletions from nt 254 to 313 (Pav3-151/313) and 313 to 383 (Pav3-151/383) resulted in a five-to eightfold reduction in viral yields in single infection, and three-to sevenfold reduction in packaging ability in coinfections, respectively. These results suggested that there are packaging motifs located between nt 254 and 313 and nt 313 and 383. The additional deletions extending from nt 383 to 497 (Pav3-151/433, Pav3-151/449, Pav3-151/474, Pav3-151/497) did not result in the further significant reduction in viral growth in single infection and in packaging ability in coinfection assays. Although deletion

from nt 497 to 531 is not lethal, deletion extending from nt 151 to 531 (Pav3-151/531) resulted in the loss of virus viability, suggesting that the sequence between nt 497 to 531 contains a packaging motif which alone can support the packaging of PAV-3. This motif probably represented the downstream border packaging motif. Surprisingly, the mutant with a deletion between nt 151 and 449 (Pav3-151/449) showed 20-fold reduction in the virus yield in VIDO R1 cells in a single infection. The reasons for this phenomenon remain unclear.

A second set of viral mutants was constructed which contained unidirectional deletions progressing from a common site at nt 531 toward the upstream border of the packaging domain (Fig. 6A). As seen in Fig. 6A, we could not isolate a viable mutant PAV-3 when deletions extended from nt 531 to 212 (Pav3-212/531). The results suggested that the packaging domain of PAV-3 existed between nt 212 and 531. The addition of DNA sequences between nt 212 and 252 (Pav3-252/531) made the virus viable, suggesting that there exists a packaging motif in this region, which alone can make the mutant virus viable (Figs. 6A and B).
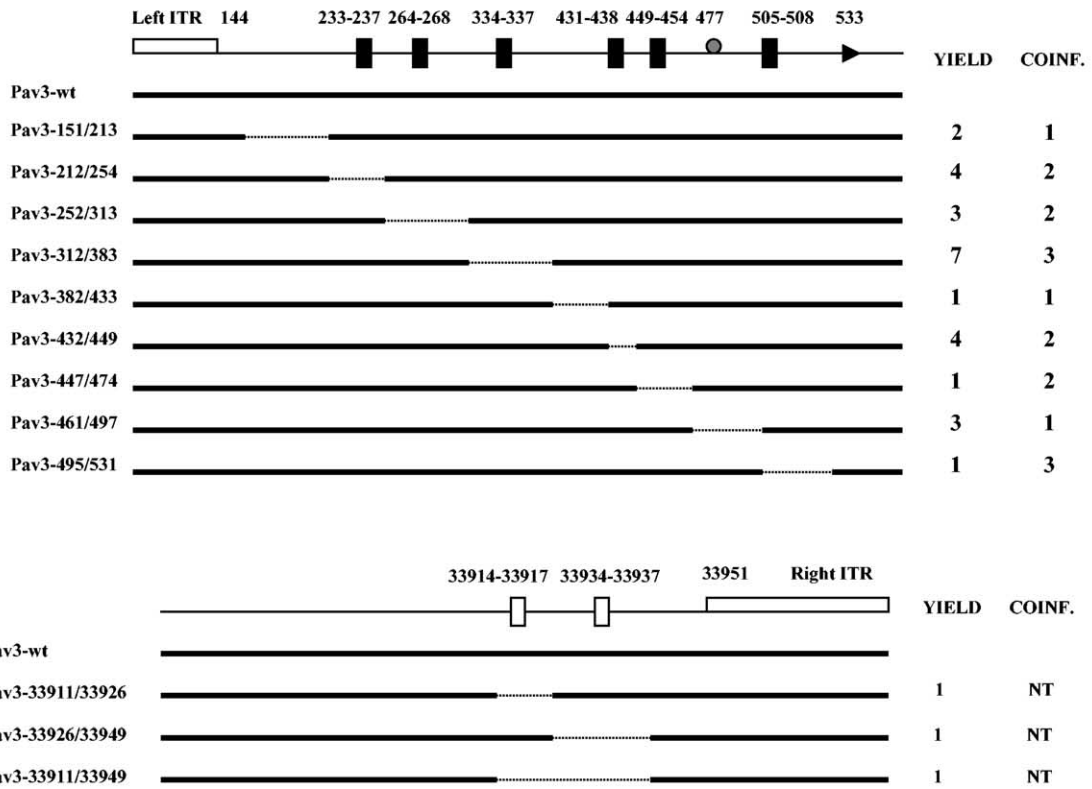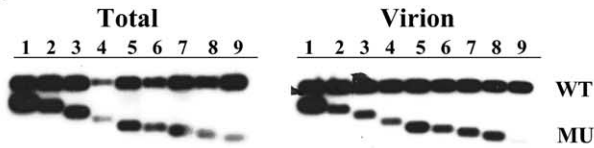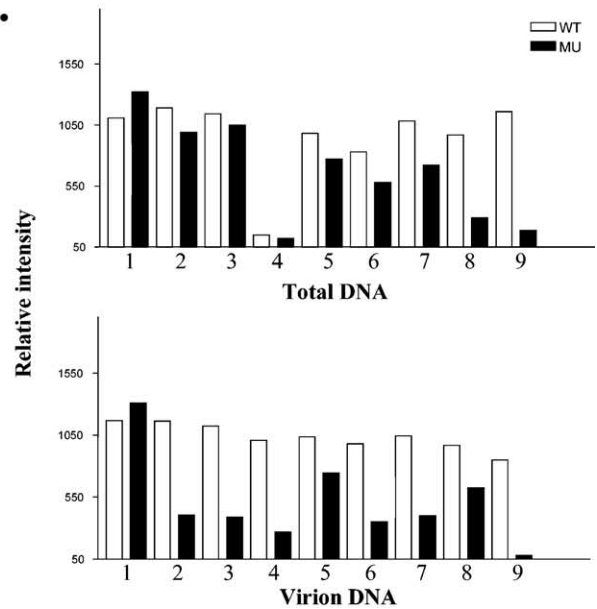
Fig. 4. Analysis of viral mutants carrying individual deletions. (A) Schematic view of viral mutants. The top of the figure shows the position of AT/GC-rich motifs (filled box); E1A cap site (filled circle) and E1A ATG (arrow head), and structure of the left terminus of PAV-3 genome. The individual deletion mutant names are given on the left. The nucleotide numbers correspond to the first nucleotides present on either side of the deletion. The deleted sequences are indicated by dotted line. Mutant virus yields (YIELD) are expressed as the fold reduction in yield relative to that of wild-type virus. Mutant virus packaging efficiency (COINF) is expressed as the fold reduction in packaged mutant DNA relative to the packaged coinfecting wild-type DNA. The data were normalized to the amount of each viral DNA (mutant and wild-type) present in total DNA. NT, not tested. (B) Southern hybridization analysis of viral DNA represented either in total DNA or in virion particles isolated from VIDO R1 cells coinfected with wild-type and the mutant viruses. Total nuclear DNA and virion DNA were digested with *Mfe*I and *Kpn*I and subsequently subjected to Southern hybridization analysis using PAV-3 left-end and fragment between nt 531 and 844 as a [^{32}P]-labeled probe. The corresponding wild-type (WT) and mutant (MU) left-end DNA fragments are indicated. The mutant viruses tested were Pav3-151/213 (lane 1), Pav3-212/254 (lane 2), Pav3-252/313 (lane 3), Pav3-312/383 (lane 4), Pav3-382/433 (lane 5), Pav3-432/449 (lane 6), Pav3-447/474 (lane 7), Pav3-461/497(lane 8), Pav3-495/531(lane 9). (C) Results of the phosphoimager scanning of DNA band intensity are shown.

This motif represented the upstream border of the packaging domain of PAV-3. The sequential addition of DNA sequences between nt 252 and 382 (Pav3-312/531, Pav3-382/531) resulted in a five- to ninefold increase in the yield and a one- to fourfold increase in the packaging ability compared with that of mutant virus Pav3-252/531 (Figs. 6A and B). These results suggested that there appears to be two packaging motifs located between nt 252 and 382. The addition of DNA sequences between nt 382 and 432 (Pav3-432/531) had no effect either on the yield or on the packaging ability of PAV-3. However, the addition of DNA sequences between nt 432 and 447 resulted in onefold increase in the virus yield and twofold increase in the packaging ability when compared with that of Pav3-432/531, suggesting that a packaging motif exists between nt 432 and 447 (Figs. 6A and B). Although there was no difference in the yield of Pav3-447/531 and Pav3-461/531 in single infection, addition of nt 447 to 461 resulted in a onefold increase in the packaging ability of Pav3-461/531. This suggested that nt 447 to 461 may contain a packaging motif.

Although Pav3-151/449, Pav3-151/433, and Pav3-151/474 showed comparable packaging ability in coinfection assays (Fig. 5), Pav3-151/449 showed a two and one-half fold more reduction in virus yield than Pav3-151/433 or Pav3-151/474 in single infection of VIDO R1 cells. To reconfirm these observations, we constructed another set of mutants with deletions progressing from a common site at nt 449 toward the upstream border of packaging domain at nt 212 (Fig. 7A). The sequential addition of DNA sequences between nt 212 and 252 (Pav3-252/449), 252 and 312 (Pav3-312/449), and 312 and 382 (Pav3-382/449) increased the packaging ability of PAV-3 correspondingly in a coinfection assay (Fig. 7A and B). These data are in agreement with that described above (Fig. 5) and confirm that packaging motifs exist in these three regions. In contrast, there was still significant reduction in the yield of Pav3-212/449 and Pav3-252/449 in VIDO R1 cells in a single infection assay (Fig. 7A). However, the addition of DNA sequences between nt 252 and 312 enhanced significantly the viral growth in VIDO R1 cells, although it made the viral packaging ability increase slightly. These data suggested that DNA sequences between nt 252 and 312 may have other unknown functions in viral life cycle which significantly affect the yield of the PAV-3.

Discussion

Adenoviruses appear to package its DNA in preformed empty capsids (D'Halluin et al., 1978a, 1978b, 1980; Edvardsson et al., 1976, 1978) by recognition of specific viral sequences by viral and cellular packaging proteins (Fujisawa and Hearing, 1994; Grable and Hearing, 1992; Schmid and Hearing, 1995, 1998). Although the identity of viral and cellular proteins that interact with packaging domain is

becoming clear (Gustin and Imperiale, 1998; Hasson et al., 1989; Schmid and Hearing, 1998; Zhang et al., 2000, 2001), the cis-acting packaging sequences appear to be conserved among the subgroups of human adenoviruses (Schmid and Hearing, 1997). However, the primary sequence of the cis-acting packaging motif(s) of CAV-2 (nonhuman adenovirus) appears to be different, suggesting that viral elements involved in the DNA packaging might have adapted to interact with species-specific cellular factors (Soudais et al., 2001). Here, we describe the construction and characterization of packaging mutants, and the sequence motifs that appear to direct PAV-3 packaging.

Although cis-acting packaging domain of adenoviruses appears to be located near the left end of the genome, it can also be functional even when present in the last 600 bp of the right end of adenovirus genome (Hammarskjold and Winberg, 1980; Hearing and Shenk, 1983; Hearing et al., 1987). Interestingly, analysis of the right end of PAV-3 genome identified two motifs containing first element (5′-TTTG-3′) of consensus sequence of cis-acting packaging motif of HAV-5 (Schmid and Hearing, 1997). Similar motifs have been shown to be part of the cis-acting packaging domain of CAV-2 (Soudais et al., 2001). However, mutant PAV-3s containing deletion of one or both motifs (5′-TTTG-3′) grew as well as wild-type virus, suggesting that these motifs are not involved in the packaging of PAV-3 genome. In contrast, analysis of PAV-3 mutants containing deletions in the left end of PAV-3 identified functional cis-acting packaging domain to 319 bp (nt 212 to 531), which showed no sequence homology to bipartite packaging motif of HAV-5 (Schmid and Hearing, 1997). Additionally, aside from AT/GC-rich character, none of the potential packaging motifs showed any primary sequence homology. These results confirm earlier observations (Soudais et al., 2001) and further suggest that primary sequence requirements for packaging motif(s) may be different for adenoviruses of different species.

Of the five known PAV serotypes (Derbyshire et al., 1975; Hirahara et al., 1990), DNA sequences of only PAV-3 (Reddy et al., 1998a,b) and PAV-5 (Nagy et al., 2001) are known. Analysis of the left end of PAV-5 genome does not contain putative cis-acting packaging motifs identified in HAV-5 (Schmid and Hearing, 1997) and CAV-2 (Soudais et al., 2001). In contrast, we could identify AT/GC-rich motifs between left ITR and ATG of E1A of PAV-5 genome. Interestingly, the number and organization of these AT/GC-rich motifs appear similar to those identified in PAV-3 (Table 2), suggesting that other porcine adenoviruses may have identical cis-acting packaging motifs. Although more data are required to draw a conclusion, it appears that adenoviruses infecting the same host may have similar packaging motifs, which will allow them to interact with viral and host-specific cellular factors.

PAV-3 packaging domain contains six AT/GC-rich elements, one of which contains consensus sequence (5′-TTTG-3′) of cis-acting packaging domain of CAV-2 (Sou-
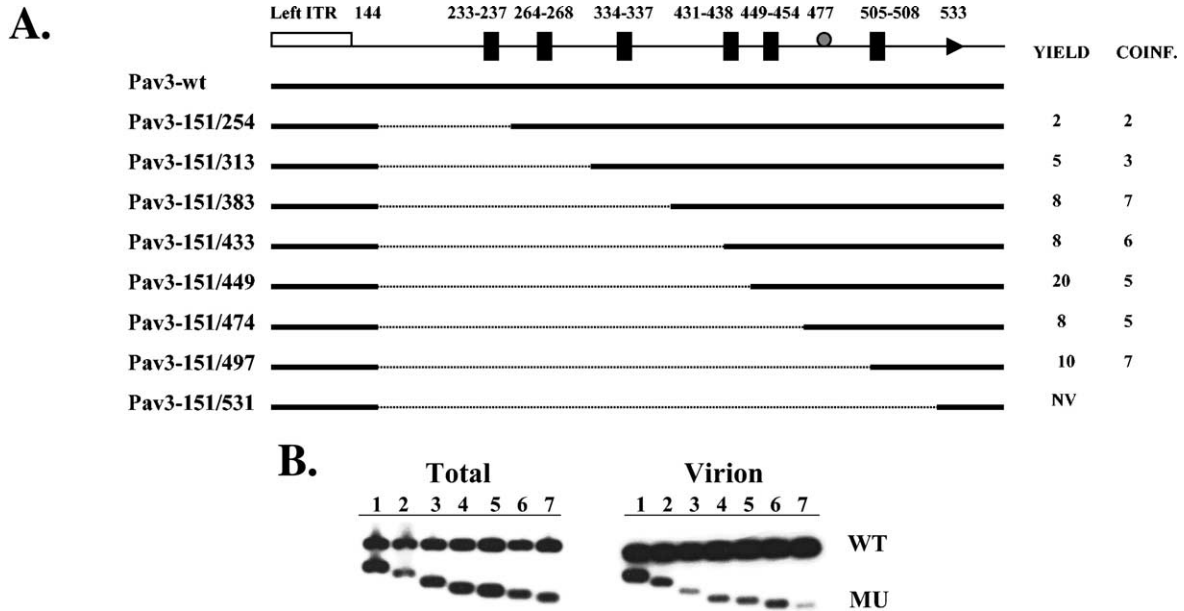
A.

B.

Fig. 5. Analysis of viral mutants carrying progressive deletions with a common start site at nt 151. (A) The schematic, mutant names, endpoints of the deletion, and in vivo packaging analysis are as described in the legend to Fig. 4A. (B) Southern hybridization analysis of total and virion DNA isolated from VIDO R1 cells coinfected with wild-type and individual mutant viruses. Southern hybridization analysis of total DNA and virion DNA was performed as described in the legend to Fig. 4B. The mutant viruses tested were Pav3-151/254 (lane 1), Pav3-151/313 (lane 2), Pav3-151/383 (lane 3), Pav3-151/433 (lane 4), Pav3-151/449 (lane 5), Pav3-151/474 (lane 6), Pav3-151/497 (lane 7). NV, nonviable virus.

dais et al., 2001). Interestingly, another packaging motif overlaps the TATA box (nt 449–454) of the E1A promoter. Although the AT/GC-rich motifs appear to be functionally redundant and have additive effect on the packaging efficiency, these motifs (individual or combination) do not appear to be functionally equivalent in VIDO R1 cells. These results are consistent with the suggestions that different packaging factors may interact with different packaging motifs depending upon the type of cells infected (Soudais et al., 2001).
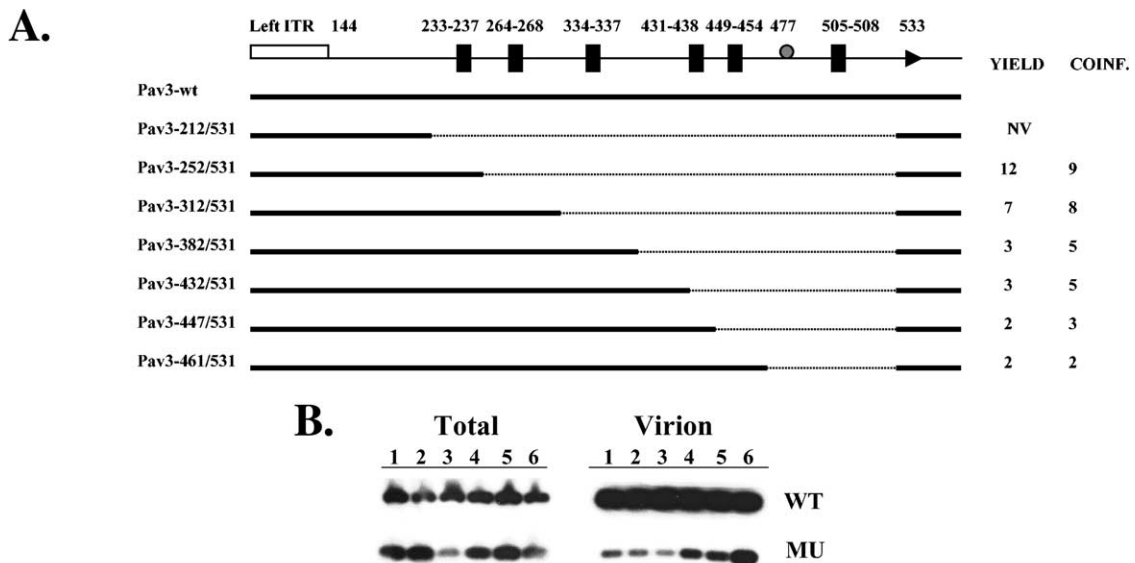
A.

B.

Fig. 6. Analysis of viral mutants carrying progressive deletions with a common start site at nt 531. (A) The schematic, mutant names, endpoints of the deletion, and in vivo packaging analysis are as described in the legend to Fig. 4A. (B) Southern hybridization analysis of total and virion DNA isolated from VIDO R1 cells coinfected with wild-type and individual mutant viruses. Southern hybridization analysis of total DNA and virion DNA was performed as described in the legend to Fig. 4B. The mutant viruses tested were Pav3-252/531(lane 1), Pav3-312/531 (lane 2), Pav3-382/531 (lane 3), Pav3-432/531 (lane 4), Pav3-447/531(lane 5), Pav3-461/531 (lane 6). NV, nonviable virus.
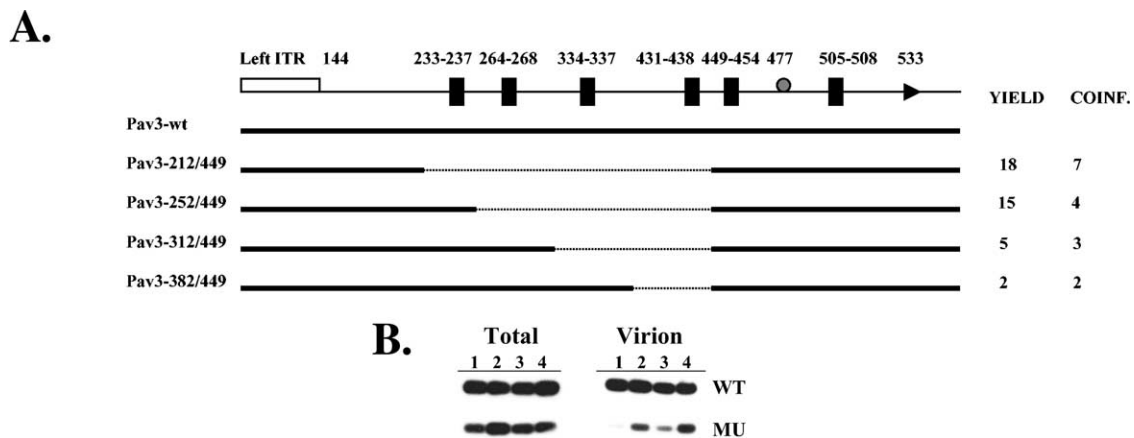
Fig. 7. Analysis of viral mutants carrying progressive deletions with a common start site at nt 449. The schematic, mutant names, endpoints of the deletion, and in vivo packaging analysis are as described in the legend to Fig. 4A. (B) Southern hybridization analysis of total and virion DNA isolated from VIDO R1 cells coinfected with wild-type and individual mutant viruses. Southern hybridization analysis of total DNA and virion DNA was performed as described in the legend to Fig. 4B. The mutant viruses tested were Pav3-212/449 (lane 1), Pav3-252/449 (lane 2), Pav3- 312/449 (lane 3), and Pav3-382/449 (lane 4).

Several mutant viruses exhibited an unexpected decrease in the virus yield in a single infection. As these mutant viruses showed comparable packaging capacity in coinfection experiments with wild-type PAV-3, the defect appeared to be in the absence of a *trans*-acting factor(s). Our results suggest that a cis-acting element required for this effect is located between nt 252 and 312. In HAV-5, the *cis*-acting packaging domain overlaps two distinct transcriptional enhancer elements. Element I specifically stimulates E1A transcription (Hearing and Shenk, 1986) upon binding of a cellular factor EF1A (Bruder and Hearing, 1989). Element I mutants can be efficiently complemented in single infection by propagation of virus in E1-expressing cells (e.g., 293 cells) (Graham et al., 1977). In contrast, element II enhances transcription from all early transcription units. Element II mutants can be efficiently complemented *in trans* by providing all of the gene products in a mixed infection with wild-type virus (Hearing and Shenk, 1986). Although the nature of the defect in these PAV-3 mutants is not known, it is possible that this region may regulate viral gene expression similar to the enhancer element II of HAV-5 E1A transcription unit (Hearing and Shenk, 1983, 1986).

Some mutant HAV-5 (Grable and Hearing, 1990) or CAV-2 (Soudais et al., 2001) viruses showed dramatic reduction in the virus yield in single infections or coinfections. In contrast, the effects of most of the deletion mutations on mutant PAV-3 yield ranged from 2- to 20-fold except on two nonviable mutant PAV-3s. It is possible that a functionally intact packaging motif(s) critical for DNA packaging is present in these mutants. Alternatively, the effect of spatial changes between individual packaging motifs may not affect virus yield in PAV-3 as severely as observed in HAV-5 (Schmid and Hearing, 1997).

Knowledge of requirements of DNA packaging of PAV-3 has important implications for the development of improved gutless adenovirus gene transfer vectors. Gutless or helper-dependent adenovirus vectors have demonstrated great promise in reducing the host immune response against virus encoded proteins and extending the expression of therapeutic gene (Balague et al., 2000; Chen et al., 1997; Cregan et al., 2000; Kim et al., 2001; Maione et al., 2000; Morral et al., 1998,1999; Morsy et al., 1998; Oka et al., 2001; Schiedner et al., 1998; Thomas et al., 2000; Zhou et al., 2001). Although a number of approaches have been developed to make gutless adenovirus vectors (Ng et al., 2001; Parks et al., 1996; Sandig et al., 2000; Umana et al., 2001; Zhou et al., 2001), all of them still leave a significant level of helper virus contamination. Based on the availability of *cis*-acting packaging domain of PAV-3, and the growth properties of PAV-3 in human cells, a system can be developed where vector DNA is specifically packaged. In this system, helper vector (containing PAV-3 packaging domain) and recombinant vector (containing PAV-3 and

Table 2
Alignment of potential packaging motifs of PAV-3 and PAV-5

Virus	Packaging motif	Sequence[a]	A/T nucleotide[b]
PAV-3	I	GCGG **AAATT** CCCG	233–237
	II	CGGG **ATTTT** GTGC	264–268
	III	CCGG **TATT** CCCC	334–337
	IV	GGTG **TATTTTTT** CCCC	431–438
	V	AGTG **TATATA** GTCC	449–454
	VI	AGAG **TTTT** CTCT	505–508
PAV-5	I	CTGG **TATTTT** CCAC	187–192
	II	TGTG **ATATT** GGAC	207–211
	III	GACC **TTTA** CCTG	217–220
	IV	ACTC **AATTTTA** CCAC	271–277
	V	GTCG **ATTTT** CCAC	321–326
	VI	TCCC **TATTTATT** CTGC	349–356

[a] AT-rich sequences are indicated in boldface type.
[b] Numbers indicate the nucleotide position relative to the left terminus of PAV-3 (Reddy et al., 1998b) or PAV-5 (Nagy et al., 2001) genomes.

HAV-5 packaging domains) will be transfected into porcine cells infected with PAV-3, leading to the production of three types of viral particles. This mixture can be used to infect human cells which will only package genomes containing HAV-5 packaging domain, thus helping to eliminate or substantially reduce the helper virus contamination.

Materials and methods

Cells and viruses

VIDO R1 cells (HAV-5 E1-expressing fetal porcine retina cells) (Reddy et al., 1999b) were grown and maintained in Eagle's minimum essential medium (MEM) supplemented with 10% fetal bovine serum (FBS). The wild-type (6618 strain) (Clarke et al., 1967) and mutant PAV-3s were propagated and titrated in VIDO R1 cells.

Construction of recombinant plasmids

A 6.814-kb Eco47-3 fragment [containing vector backbone plus the left (nt 1–2192) and right (nt 31499–34094) termini of the PAV-3 genome] isolated from pFPAV200 (Reddy et al., 1999a) was religated, creating plasmid pPAV3.Eco47-3 (Fig. 2A). Nucleotide numbers of the PAV-3 genome referred to in this article are given according to GenBank Accession No. AF083132. This plasmid DNA containing both the ends of PAV-3 genome was used as template in PCR amplifications using specific primers (Table 1) to create specific deletion between left ITR and ATG of E1A gene (Reddy et al., 1998b). The following conditions were used for PCR in a total volume of 50 μl: 0.5 μg of template DNA, 1$\times$ PCR buffer [10 mM KCl, 10 mM $(NH_4)_2SO_4$, 20 mM Tris–Cl (pH 8.75), 2 mM $MgSO_4$, 0.1% Triton X-100, 0.1 mg/ml BSA; Stratagene], 0.4 mM dNTPs, 10 pmol of each primer, 2.0 U of cloned *pfu* DNA polymerase (Stratagene). The cycling conditions were 94°C for 2 min to denature the DNA, followed by 30 cycles consisting of 94°C for 40 s, 50°C for 40 s, 72°C for 40 s, and finally, extention at 72°C for 2 min. The products of PCR were separated on a 2% agarose gel and visualized by ethidium bromide (EtBr) staining.

To construct recombinant transfer plasmids containing the deletions between left ITR and ATG of E1A gene of PAV-3 (Reddy et al., 1999b), first the DNA fragments amplified using primer pairs P1-P3, P1-P5, P1-P7, P1-P9, P1-P11, P1-P13, P1-P15, P1-P17, and P1-P19 were digested with *Bam*HI and *Mfe*I. Second, the DNA fragments amplified using primer pairs P2-P4, P2-P6, P2-P8, P2-P10, P2-P12, P2-P14, P2-P16, P2-P18, P2-P20 were digested with *Mfe*I and *Eco*RV. The appropriate *Bam*HI-*Mfe*I and *Mfe*I-*Eco*RV DNA fragments were ligated to *Bam*HI-*Eco*RV-digested pPAV3.Eco47-3 in a three-way ligation, thus creating the recombinant transfer plasmids containing the

desired deletions between left-end ITR and ATG codon of E1A gene of PAV-3 (Figs. 4A, 5A, 6A, and 7A).

To construct the recombinant plasmids containing the deletions between right-end ITR and E4 gene of PAV-3, first the DNA fragments amplified using primer pairs PR1-PR3 and PR1-PR5 were digested with *Hpa*I and *Mfe*I. Second, the DNA fragments amplified using primer pairs PR2-PR4 and PR2-PR6 were digested with *Mfe*I and *Pac*I. The appropriate *Hpa*I-*Mfe*I and *Mfe*I-*Pac*I DNA fragments were ligated to *Hpa*I-*Pac*I-digested pPAV3.Eco47-3 in a three-way ligation, thus creating the recombinant transfer plasmid(s) containing desired deletions between E4 and right-end ITR (Fig. 4A).

The plasmids containing the full-length genome of PAV-3 with deletions in the putative packaging domain were generated by homologous recombination in *E. coli* BJ5183 (Chartier et al., 1996) between Eco47-3-linearized individual recombinant transfer plasmid and the genomic DNA from wild-type PAV-3 (Fig. 2B). These plasmids were characterized by restriction endonuclease analysis. The endpoints of deletion plasmids containing the desired deletions between E4 and the right ITR (Fig. 4A) were determined by nucleotide sequence analysis.

Isolation of PAV-3 mutants

VIDO R1 cell monolayers were seeded in a 35-mm-diameter dish and were transfected with 5 μg of *Pac*I-digested individual full-length plasmid DNA using the Lipofectin methods according to the instructions of manufacturer (Invitrogen). After 10 to 15 days of incubation at 37°C, the transfected cells were collected and freeze thawed three times. The lysates were used to infect the freshly prepared VIDO R1 cells until cytopathic effect appeared. Finally, the recombinant viruses were characterized by PCR and restriction analysis and then expanded and titrated on VIDO R1 cells.

Determination of virus yields and packaging efficiency

All viral infections were performed at an multiplicity of infection (m.o.i.) of 5 plaque-forming units (PFU) per cell at 37°C for 1 h. The cells were washed and fresh medium was added. For the determination of viral yield in single-virus infections, infected VIDO R1 cells were harvested 48 h after infection and then lysed by three cycles of freezing and thawing. The infectious virus yields in cleared lysates were determined by plaque assay on VIDO R1 cells. The data presented for virus yields from single infections represent the averages of three independent experiments.

Packaging efficiency of the mutant viruses was determined by coinfection of VIDO R1 cells with both the mutant and the wild-type PAV-3, according to the method described earlier (Grable and Hearing, 1990, 1992), with little modification. VIDO R1 cells were infected with 5 PFU

of each of the viruses per cell as described above. Forty-eight hours postinfection, one-half of the cells were used to isolate high-molecular-weight DNA, and the other half of the cells were used to prepare viral DNA from virions. For the isolation of infected cell high-molecular-weight DNA, the cells were lysed by the addition of Nonidet P-40 to 0.4%, and then digested with proteinase K at 50°C for at least 2 h. The high-molecular-weight DNA was isolated as described previously (Sambrook et al., 1989). For the isolation of viral DNA from virions, infected cells were pelleted and suspended in lysis buffer [20 mM Tris–Cl (pH 8.0), 0.2% deoxycholate, 10% ethanol]. After incubation for 60 min at room temperature, the lysate was cleared at 10,000 g for 30 min. The supernatant was adjusted to 2 mM $CaCl_2$ and 2 mM $MgCl_2$, and was digested with 40 μg of RNase A per milliliter and 10 μg of DNase I per milliliter at 37°C for 30 min. The reaction was stopped by the addition of EDTA and EGTA to a final concentration of 50 mM each. Virus particles were lysed by the addition of Sarkosyl to 0.5%, and the samples were digested with 1 mg of proteinase K per milliliter at 50°C for 1 to 2 h. After phenol and chloroform extraction, the viral DNA was precipitated with ethanol. The DNAs isolated from cells or virions were digested with *Mfe*I and *Kpn*I and then analyzed by Southern hybridization.

Southern hybridization

The *Mfe*I- and *Kpn*I-digested DNAs were separated on 1.5% agarose gel and then transferred to Gene Screen Plus hybridization transfer membrane (Perkin–Elmer Life Science) by high salt capillary transfer method according to the instructions of the manufacturer. The 314-bp DNA fragment corresponding to nt 531–844 was amplified by PCR with primers P2 and P20, labeled with [^{32}P]-dCTP by the random primer method using Random Primers DNA labeling system (Invitrogen), and used as a probe in Southern hybridization analysis. The blots were prehybridized in ULTRAhyb ultrasensitive hybridization buffer (Ambion RNA) at 42°C for 30 min, and then [^{32}P]- labeled probes were added. Hybridization was performed at 42°C overnight. After extensively washing with 0.1× SSC and 0.1% SDS, the blots were exposed to X-ray film (Kodak) without an intensifying screen. The bands in autoradiograms were scanned and their relative intensities were determined and analyzed by Computing Densitometer using phosphoimager program. The data presented for packaging efficiency based on coinfection experiments represent the averages of three independent experiments.

Acknowledgments

References

Balague, C., Zhou, J., Dai, Y., Alemany, R., Josephs, S.F., Andreason, G., Hariharan, M., Sethi, E., Prokopenko, E., Jan, H.Y., Lou, Y.C., Hubert-Leslie, D., Ruiz, L., Zhang, W.W., 2000. Sustained high-level expression of full-length human factor VIII and restoration of clotting activity in hemophilic mice using a minimal adenovirus vector. Blood 95, 820–828.

Bruder, J.T., Hearing, P., 1989. Nuclear factor EF-1A binds to the adenovirus E1A core enhancer element and to other transcriptional control regions. Mol. Cell Biol. 9, 5143–5153.

Chartier, C., Degryse, E., Gantzer, M., Dieterle, A., Pavirani, A., Mehtali, M., 1996. Efficient generation of recombinant adenovirus vectors by homologous recombination in *Escherichia coli*. J. Virol. 70, 4805–4810.

Chen, H.-H., Mack, L.M., Kelly, R., Ontell, M., Kochanek, S., Clemens, P.R., 1997. Persistence in muscle of an adenoviral vector that lacks all viral genes. Proc. Natl. Acad. Sci. USA 94, 1645–1650.

Clarke, M.C., Sharpe, H.B., Derbyshire, J.B., 1967. Some characteristics of three porcine adenoviruses. Arch. Gesamte Virusforsch. 21, 91–97.

Cregan, S.P., MacLaurin, J., Gendron, T.F., Callaghan, S., Park, D.S., Parks, R.J., Graham, F.L., Morley, P., Slack, R.S., 2000. Helper-dependent adenovirus vectors: their use as a gene delivery system to neurons. Gene Ther. 14, 1200–1209.

Daniell, E., 1976. Genome structure of incomplete particles of adenovirus. J. Virol. 19, 685–708.

Derbyshire, J.B., Clarke, M.C., Collins, A.P., 1975. Serological and pathogenicity studies with some unclassified porcine adenoviruses. J. Comp. Pathol. 85, 437–443.

D'Halluin, J.C., Martin, G.R., Torpier, G., Boulanger, P.A., 1978a. Adenovirus type 2 assembly analyzed by reversible cross-linking of labile intermediates. J. Virol. 26, 357–363.

D'Halluin, J.C., Milleville, M., Boulanger, P.A., Martin, G.R., 1978b. Temperature-sensitive mutant of adenovirus type 2 blocked in virion assembly: accumulation of light intermediate particles. J. Virol. 26, 344–356.

D'Halluin, J.C., Milleville, M., Martin, M.R., Boulanger, P., 1980. Morphogenesis of human adenovirus type 2 studied with fiber- and fiber and penton base-defective temperature-sensitive mutants. J. Virol. 33, 88–99.

D'Halluin, J.C., 1995. Virus assembly. Curr. Top. Microbiol. Immunol. 199, 47–66.

Edvardsson, B., Everitt, E., Jornvall, H., Prage, L., Philipson, L., 1976. Intermediates in adenovirus assembly. J. Virol. 19, 533–547.

Edvardsson, B., Ustacelebi, S., Williams, J., Philipson, L., 1978. Assembly intermediates among adenovirus type 5 temperature-sensitive mutants. J. Virol. 25, 641–651.

Fujisawa, H., Hearing, P., 1994. Structure, function and specificity of the DNA packaging signals in double-stranded DNA viruses. Semin. Virol. 5, 5–13.

Grable, M., Hearing, P., 1990. Adenovirus type 5 packaging domain is composed of a repeated element that is functionally redundant. J. Virol. 64, 2047–2056.

Grable, M., Hearing, P., 1992. *cis* and *trans* requirements for the selective packaging of adenovirus type 5 DNA. J. Virol. 66, 723–731.

Graham, F.L., Smiley, J., Russell, W.C., Nairu, R., 1977. Characteristics of a human cell line transformed by DNA from adenovirus type 5. J. Gen. Virol. 36, 59–72.

Gustin, K.E., Imperiale, M.J., 1998. Encapsidation of viral DNA requires the adenovirus L1 52/55-kilodalton protein. J. Virol. 72, 7860–7870.

Hammarskjold, M.L., Winberg, G., 1980. Encapsidation of adenovirus 16 DNA is directed by a small DNA sequence at the left end of the genome. Cell. 20, 787–795.

Hasson, T.B., Soloway, P.D., Ornelles, D.A., Doerfler, W., Shenk, T., 1989. Adenovirus L1 52- and 55-kilodalton proteins are required for assembly of virions. J. Virol. 63, 3612–3621.

Hearing, P., Samulski, R.J., Wishart, W.L., Shenk, T., 1987. Identification of a repeated sequence element required for efficient encapsidation of the adenovirus type 5 chromosome. J. Virol. 61, 2555–2558.

Hearing, P., Shenk, T., 1983. The adenovirus type 5 E1A transcriptional control region contains a duplicated enhancer element. Cell 33, 695–703.

Hearing, P., Shenk, T., 1986. The adenovirus type 5 E1A enhancer contains two functionally distinct domains: one is specific for E1A and the other modulates all early units in *cis*. Cell. 45, 229–236.

Hirahara, T., Yasuhara, H., Matsui, O., Yamanaka, M., Tanaka, M., Fukuyama, S., Izumida, A., Yoshiki, K., Kodama, K., Nakai, M., Sasaki, N., 1990. Isolation of porcine adenovirus from the respiratory tract of pigs in Jpn.. J. Vet. Sci. 52, 407–409.

Kim, I.H., Jozkowicz, A., Piedra, P.A., Oka, K., Chan, L., 2001. Life time correction of genetic deficiency in mice with a single injection of helper-dependent adenoviral vector. Proc. Natl. Acad. Sci. USA 98, 13282–13287.

Kosturko, L.D., Sharnick, S.V., Tibbetts, C., 1982. Polar encapsidation of adenovirus DNA: cloning and DNA sequence of the left end of adenovirus type 3. J. Virol. 43, 1132–1137.

Maione, D., Wiznerowicz, M., Delmastro, P., Cortese, R., Ciliberto, G., Monica, N. La., Savino, R., 2000. Prolonged expression and effective readministration of erythropoietin delivered with a fully deleted adenoviral vector. Hum. Gene Ther. 11, 859–868.

Morral, N., O'Neal, W., Rice, K., Leland, M., Kaplan, J., Piedra, P.A., Zhou, H., Parks, R.J., Velji, R., Aguilar-Córdova, E., Wadsworth, S., Graham, F.L., Kochanek, S., Carey, K.D., Beaudet, A.L., 1999. Administration of helper-dependent adenoviral vectors and sequential delivery of different vector serotype for long-term liver directed gene transfer in baboons. Proc. Natl. Acad. Sci. USA 96, 12816–12821.

Morral, N., Parks, R.J., Zhou, H., Langston, C., Schiedner, M., Quinones, J., Graham, F.L., Kochanek, S., Beaudet, A.L., 1998. High doses of a helper-dependent adenoviral vector yield supraphysiological levels of α1-antitrypsin with negligible toxicity. Hum. Gene Ther. 9, 2709–2716.

Morsy, M.A., Gu, M., Motzel, S., Zhao, J., Lin, J., Su, Q., Allen, H., Franlin, L., Parks, R.J., Graham, F.L., Kochanek, S., Bett, A.J., Caskey, C.T., 1998. An adenoviral vector deleted for all viral coding sequences results in enhanced safety and extended expression of a leptin transgene. Proc. Natl. Acad. Sci. USA. 95, 7866–7871.

Nagy, M., Nagy, E., Tuboly, T., 2001. The complete nucleotide sequence of porcine adenovirus serotype 5. J. Gen. Virol. 82, 525–529.

Ng, P., Beauchamp, C., Evelegh, C., Parks, R., Graham, F.L., 2001. Development of a FLP/frt system for generating helper-dependent adenoviral vectors. Mol. Ther. 3, 809–815.

Oka, K., Pastore, L., Kim, I.-H., Merched, A., Nomura, S., Lee, H.-J., Merched-Sauvage, M., Arden-Riley, C., Lee, B., Finegold, M., Beaudet, A., Chan, L., 2001. Long-term stable correction of low-density lipoprotein receptor-deficient mice with a helper-dependent adenoviral vector expressing the very low-density lipoprotein receptor. Circulation 103, 1274–1281.

Parks, R.J., Chen, L., Anton, M., Sankar, U., Rudnicki, M.A., Graham, F.L., 1996. A helper-dependent adenovirus vector system: removal of helper virus by Cre-mediated excision of the viral packaging signal. Proc. Natl. Acad. Sci. USA 93, 13565–13570.

Reddy, P.S., Idamakanti, N., Babiuk, L.A., Mehtali, M., Tikoo, S.K., 1999b. Porcine adenovirus-3 as a helper-dependent expression vector. J. Gen. Virol. 80, 2909–2916.

Reddy, P.S., Idamakanti, N., Hyun, B.H., Tikoo, S.K., Babiuk, L.A., 1999a. Development of porcine adenovirus-3 as an expression vector. J. Gen. Virol. 80, 563–570.

Reddy, P.S., Idamakanti, N., Song, J.Y., Lee, J.B., Hyun, B.H., Park, J.H., Cha, S.H., Bae, Y.T., Tikoo, S.K., Babiuk, L.A., 1998b. Nucleotide sequence and transcription map of porcine adenovirus type 3. Virology 251, 414–426.

Reddy, P.S., Idamakanti, N., Song, J.Y., Lee, J.B., Hyun, B.H., Park, J.H., Cha, S.H., Tikoo, S.K., Babiuk, L.A., 1998a. Sequence and transcription map analysis of early region-1 of porcine adenovirus type-3. Virus Res. 58, 97–106.

Robinson, C.C., Tibbetts, C., 1984. Polar encapsidation of adenovirus DNA: evolutionary variants reveal dispensable sequences near the left ends of Ad3 genomes. Virology 137, 276–286.

Russell, W.C., 2000. Update on adenovirus and its vectors. J. Gen. Virol. 81, 2573–2604.

Sambrook, J., Fritsch, E.F., Maniatis, T., 1989. Molecular Cloning: A Laboratory Manual, second ed. Cold Spring Harbor Laboratory Press, Cold Spring Harbor, NY.

Sandig, V., Youil, R., Bett, A.J., Franlin, L.L., Oshima, M., Maione, D., Wang, F., Metzker, M.L., Savino, R., Caskey, C.T., 2000. Optimization of the helper-dependent adenovirus system for production and potency in vivo. Proc. Natl. Acad. Sci. USA 97, 1002–1007.

Schiedner, G., Morral, N., Parks, R.J., Wu, Y., Koopmans, S.C., Langston, C., Graham, F.L., Beaudet, A.L., Kochanek, S., 1998. Genomic DNA transfer with a high-capacity adenovirus vector results in improved in vivo gene expression and decreased toxicity. Nat. Genet. 18, 180–183.

Schmid, S.I., Hearing, P., 1995. Selective encapsidation of adenovirus DNA. Curr. Top. Microbiol. Immunol. 199, 67–80.

Schmid, S.I., Hearing, P., 1997. Bipartite structure and functional independence of adenovirus type 5 packaging elements. J. Virol. 71, 3375–3384.

Schmid, S.I., Hearing, P., 1998. Cellular components interact with adenovirus type 5 minimal DNA packaging domains. J. Virol. 72, 6339–6347.

Soudais, C., Boutin, S., Kremer, E.J., 2001. Characterization of *cis*-acting sequences involved in canine adenovirus packaging. Mol. Ther. 3, 631–640.

Tibbetts, C., 1977. Viral DNA sequences from incomplete particles of human adenovirus type 7. Cell 12, 243–249.

Thomas, C.E., Schiedner, G., Kochanek, S., Castro, M.G., Lowenstein, P.R., 2000. Peripheral infection with adenovirus causes unexpected long-term brain inflammation in animals injected intracranially with first-generation, but not with high-capacity, adenovirus vectors: toward realistic long-term neurological gene therapy for chronic diseases. Proc. Natl. Acad. Sci. USA 97, 7482–7487.

Umana, P., Gerdes, C.A., Stone, D., Davis, J.R.E., Ward, D., Castro, M.G., Lowenstein, P.R., 2001. Efficient FLPe recombinase enables scalable production of helper-dependent adenoviral vectors with negligible helper-virus contamination. Nat. Biotechnol. 19, 582–585.

Zhang, W., Imperiale, M.J., 2000. Interaction of the adenovirus IVa2 protein with viral packaging sequences. J. Virol. 74, 2687–2693.

Zhang, W., Low, J.A., Christensen, J.B., Imperiale, M.J., 2001. Role for the adenovirus IVa2 protein in packaging of viral DNA. J. Virol. 75, 10446–10454.

Zhou, H., Zhao, T., Pastore, L., Nageh, M., Zheng, W., Rao, X.M., Beaudet, A.L., 2001. A Cre-expressing cell line and an E1/E2a double-deleted virus for preparation of helper-dependent adenovirus vector. Mol. Ther. 3, 613–22.

Zou, L., Yuan, X., Zhou, H., Lu, H., Yang, K., 2001. Helper-dependent adenoviral vector-mediated gene transfer in aged rat brain. Hum. Gene Ther. 12, 181–191.